Aalto University

Zhang, Yanpu; Li, Fei; Valenzuela, Luis D.; Sammalkorpi, Maria; Lutkenhaus, Jodie L.

Effect of Water on the Thermal Transition Observed in Poly(allylamine hydrochloride)–Poly(acrylic acid) Complexes

Macromolecules

Article

Effect of Water on the Thermal Transition Observed in Poly(allylamine hydrochloride)−Poly(acrylic acid) Complexes

Yanpu Zhang,[†] Fei Li,[†] Luis D. Valenzuela,[†] Maria Sammalkorpi,[§] and Jodie L. Lutkenhaus[*,†,‡]

[†]Artie McFerrin Department of Chemical Engineering and [‡]Department of Materials Science and Engineering, Texas A&M University, College Station, Texas 77843, United States
[§]Department of Chemistry, Aalto University, P.O. Box 16100, 00076 Aalto, Finland

S *Supporting Information*

ABSTRACT: Here, we present the thermal behavior of polyelectrolyte complexes (PECs) containing weak polyelectrolytes poly(allylamine hydrochloride) (PAH) and poly(acrylic acid) (PAA) as influenced by water content and complexation pH. Modulated differential scanning calorimetry (MDSC) reveals a glass-transition-like thermal transition (T_{tr}) that decreases in value with increasing hydration and with decreasing complexation pH. We show the collapse of all T_{tr} values into a single master curve when plotted against the ratio of water molecules per intrinsic (PAH$^+$−PAA$^-$) ion pair for all pH values explored. Remarkably, this master curve is linear when the natural log of the water to intrinsic ion pair ratio is plotted against the inverse of T_{tr}. This strongly indicates that the thermal transition is heavily influenced by water at the intrinsic ion pair site. Other water−solvent mixtures are also explored, for which T_{tr} appears to depend only on water content, regardless of the added solvent. These results suggest that water plays a dual role in PAH−PAA complex: first by participating in the hydrogen-bonding network within and second by plasticizing the PEC. A hypothesis for the thermal transition is proposed in which hydrated PECs undergo a two-step thermal transition caused by an initial restructuring of the water−polyelectrolyte hydrogen-bonding network, followed by chain relaxation.
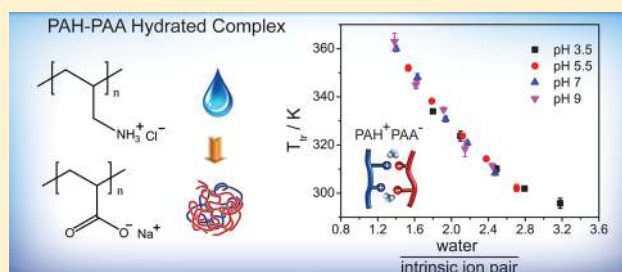
INTRODUCTION

Polyelectrolyte complexes (PECs), prepared via mixing oppositely charged polymer solutions together, have attracted increasing attention in recent years in terms of fundamental phase behavior.[1−7] PECs can be processed into films[8,9] and extrudable shapes,[10,11] thus opening up a broad range of applications. Further, PEC structure is finely controlled by complexation conditions and parameters such as polymer charge density and molecular weight, ionic strength, and pH value.[12,13] Once formed, PECs act as "smart" materials in which they respond to various external stimuli including ionic strength, pH, and temperature.[10,14,15] These stimuli-responsive behaviors are almost always observed in the hydrated state because dry PECs are somewhat glassy and intractable.[16] Of these external stimuli, temperature is particularly intriguing because the origin of temperature effects on PECs is not immediately obvious as compared to ionic strength or pH effects.

For over a decade, it has been known that *hydrated* polyelectrolyte multilayers or layer-by-layer (LbL) films undergo a "glass-melt" transition with some assigning this temperature as the glass-melt temperature T_m or the glass transition temperature T_g.[17−19] This thermal transition has been further leveraged to release cargo from capsules and induce Rayleigh instabilities in microtubes.[20−24] General observations indicate hydrated polyelectrolyte multilayers

soften and that polymer chains relax as they are heated through the transition.[18,19,25,26] Most literature in this area focuses on hydrated polyelectrolyte multilayers, with recent work showing that hydrated PECs have a similar tendency.[10]

On the other hand, *dried* polyelectrolyte multilayers and complexes have markedly different behavior upon comparison with *hydrated* ones, which suggests that water plays a critical role in the thermal transition. Shamoun et al. reported no distinctive thermal transition for dried extruded complexes of strong polyelectrolytes poly(diallyldimethylammonium chloride) (PDAC) and poly(sodium 4-styrenesulfonate) (PSS).[10] Huglin et al. found that dried PECs consisting of poly(4-vinylpyridinium chloride) and poly[sodium(2-acrylamido-2-methylpropanesulfonate)] possessed no discernible T_g due to the high density of ionic cross-linking.[27] Electrospun weak polyelectrolyte poly(allylamine hydrochloride)−poly(acrylic acid) (PAH−PAA) PEC fibers exhibited no T_g as well.[15] In our own work we have demonstrated that PAH/PAA multilayers also exhibit no T_g and instead undergo thermal cross-linking.[28,29] These findings show that dried PECs generally do not possess a T_g because of extensive ion-pairing, which results in a highly physically cross-linked PEC network.

Remarkably in the presence of water, these same PEC systems exhibit the glass-melt thermal transition which we will call here simply the thermal transition, T_{tr}. Shamoun et al. demonstrated that hydrated PDAC–PSS complexes have a T_g that is dependent on ionic strength, but the effect of water composition on the T_g was not explored.[10] Separately, we have demonstrated that hydrated PDAC/PSS multilayers also have a salt-dependent thermal transition.[30,31] These results are consistent with the pioneering work of Michaels, who described that PECs were brittle when dry but "leathery or rubberlike" when hydrated.[16] These results suggest that water acts as a plasticizer, possibly lowering the PEC's or multilayer's thermal transition temperature from an unobservable value in the dry state to an observable value in the hydrated state. This is supported by observations of PDAC–PSS complexes' dehydration under osmotic stress[32] and water–polyelectrolyte interactions in PDAC/PSS multilayers.[33]

Our recent experimental and simulational findings on the PDAC/PSS system suggest that the thermal transition is not a classical glass transition but is rather initiated by rearrangement of water molecules around the polyanion.[34] It is thus hypothesized that as the hydrogen bond lifetime between water–polyanion shortens, the polyelectrolyte chains relax, leading to the observed glass-transition-like behavior. Elsewhere, it has been discussed that the transition may arise from the breaking and reformation of polyelectrolyte–polyelectrolyte ion pairs (here called "intrinsic ion pairs") facilitated by salt-doping and water.[10] In both cases, water is considered a key factor, although its exact role remains unclear. Therefore, a thorough understanding of water's role in the transition, whether it proceeds by the former, latter, or both mechanisms, is of fundamental importance and motivates the present study.

There also remains a question as to whether PECs of weak polyelectrolytes undergo a transition by the same mechanism. The thermal properties of hydrated complexes containing weak polyelectrolytes are presently not well described, and such information could yield valuable insight into water's influence. An added complication rises from the pH of complexation altering the polyelectrolyte charge density and the resulting PEC structure.[35,36] Earlier we investigated PAH/PAA multilayers and microtubes, in which a pH-dependent T_{tr} was observed using both quartz crystal microbalance with dissipation (QCM-D), modulated differential scanning calorimetry (MDSC), and microscopy.[21,37] Motivated by these results, we hypothesized that hydrated complexes would show distinct thermal transitions and would be affected by the complexation pH value and hydration conditions.

Here, the thermophysical properties of dried and hydrated PAH–PAA complexes are investigated. This weak polyelectrolyte system is chosen because information regarding its thermal transition is sparse and because the system provides a unique opportunity to explore pH and ionization effects not normally accessible in strong polyelectrolyte systems. In experiments, PAH–PAA complexes are prepared at varying complexation pH values. The degree of PAA ionization and the PEC composition are analyzed using Fourier-transform infrared (FTIR) and proton nuclear magnetic resonance (^{1}H NMR) spectroscopy, respectively. The thermal behavior of PECs with varying hydration is studied using MDSC. The effect of water mixtures with 1-propanol, 1,2-propanediol, 1,3-propanediol, and urea on the T_{tr} is also examined. A connection between the thermal transition and water–intrinsic ion pair interactions is made and discussed in the broader context of a proposed two-step mechanism for the thermal transition.

■ EXPERIMENTAL SECTION

Materials. Poly(allylamine hydrochloride) (PAH, M_w = 120 000–200 000 g mol^{-1}, 40 wt % solution) was purchased from Polysciences, Inc., and poly(acrylic acid) (PAA, M_w = 100 000 g mol^{-1}, 35 wt % in H$_2$O) was obtained from Sigma-Aldrich. Both polyelectrolytes were used as received without any further treatment. Deuterium chloride 35% in D$_2$O solution used in proton nuclear magnetic resonance (^{1}H NMR) was also purchased from Sigma-Aldrich. 2,2-Dimethyl-2-silapentane-5-sulfonate (DSS) was kindly provided by the Texas A&M University NMR Facility. The water used in all experiments was Milli-Q water with resistivity 18.2 MΩ·cm.

Preparation of Polyelectrolyte Complexes. Individual solutions of PAH or PAA were prepared at concentrations of 100 mM with respect to their repeat unit. 1 M HCl or NaOH was used to adjust the solution pH to desired values. 50 mL of PAH and PAA at matching pH values were mixed, with PAH being added rapidly to PAA under constant stirring. The complex was dialyzed against water at matching pH for 4 days. The complex mixture was decanted after centrifugation at 8500 rpm for 10 min. Then the complex was air-dried for ca. 12 h. This preliminary air-dried complex was finely ground into a powder, then placed in a vacuum oven at 303 K for another 7 days, and stored in a desiccator until further characterizations. This yielded the "dried" PEC, although it is acknowledged that it is impossible to remove all bound water. A PEC prepared at pH m will be referred to as a "(PAH–PAA)$_m$ PEC".

Modulated Differential Scanning Calorimetry (MDSC). MDSC (Q200, TA Instruments) was performed on PECs using a heat–cool method unless otherwise stated. The sample mass ranged between 5 and 10 mg, depending on sample availability. Dried samples were loaded into a Tzero aluminum pan (TA Instruments) and held at 313 K isothermally under nitrogen purge (50 mL min^{-1}) for 60 min prior to the scan to further remove any remaining water. The dried sample was heated up to 573 K from 313 K at a rate of 10 K min^{-1} followed by cooling at the same rate for two heat–cool cycles.

Tzero pans and hermetic lids were used for hydrated samples. Hydrated samples were prepared by weighing the dried complex in the Tzero pans and adding water at matching assembly pH using a microliter syringe. The samples were then dried at room temperature until the desired hydration content (15.3, 17.4, 20, 21.9, or 24.2 wt %) was reached. This hydration value represents the known amount of water added to the dried PEC and not the precise water content in the PEC. The pans were subsequently sealed with Tzero hermetic lids and left at room temperature for 24 h for equilibration before measurements. Hydrated samples were ramped from 278 to 388 K at a rate of 2 K min^{-1} with an amplitude of 1.272 K and a period of 60 s. Measurements were conducted under a 50 mL/min nitrogen purge. All MDSC thermograms are shown in the "exotherm down" format, and all data reported here correspond to the second heating cycle unless otherwise noted. The T_{tr}/T_g was taken as the inflection point of MDSC thermogram. Three different measurements were run for each data point, and the standard deviation was taken as the error estimate.

Fourier Transform Infrared Spectroscopy. The chemical structure of the complex was investigated by attenuated total reflectance Fourier transform infrared spectroscopy (ATR-FTIR, Thermo, Nicolet Nexus 6700) using a Quest diamond single-bounce ATR attachment (Specac). For each sample, ca. 5 mg of PEC powder was placed on the sample stage to cover the ATR crystal. Spectra were taken by averaging 64 scans over a range of 600 cm^{-1} up to 4000 cm^{-1}, at a resolution of 2 cm^{-1}. All samples were kept in a desiccator prior to FTIR spectroscopy.

Proton Nuclear Magnetic Resonance Spectroscopy. Proton nuclear magnetic resonance (^{1}H NMR) spectroscopy (500 MHz proton frequency, Varian Inova 500 spectrometer) was employed to measure the composition of PAH–PAA complexes as follows: 10 mg of dried complex sample was dissolved in 0.7 mL of deuterium chloride in an NMR tube. 20 μL of 2 mg/mL DSS was added into the

NMR tube as a standard internal reference just prior to recording the spectra.

RESULTS

PAH−PAA complexes at stoichiometric mixing conditions and at pH values varying from 1 to 11 were prepared (Figure S1). Complex precipitates easily formed between pH 3 and pH 9, whereas more extreme pH values yielded almost no precipitate. For this reason, we selected pH values of 3.5, 5.5, 7, and 9 for further investigation; these values also match prior studies on PAH/PAA layer-by-layer assemblies,[35,37] which allows for comparison with PECs. The complexes were then dialyzed, separated by centrifugation, and dried for further use.

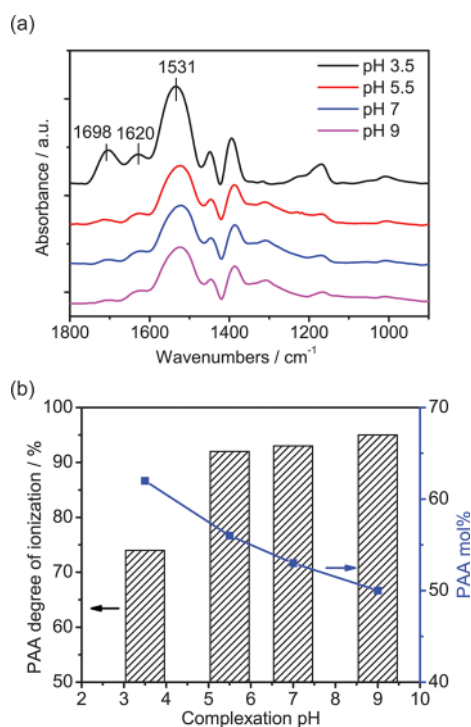Figure 1a shows ATR-FTIR spectra of the PAH−PAA complex precipitate powders. Two distinct absorption bands

Figure 1. (a) FTIR spectra and (b) PAA degree of ionization and PAA mol % (by repeat unit) for PAH−PAA complexes prepared from pH 3.5, 5.5, 7, and 9 solutions. Initial mixing ratio was 1:1 PAH to PAA by repeat unit, and PECs were separated by dialysis and centrifugation.

related to PAA carboxylic acid functional groups were observed at 1698 cm^{-1} (C=O stretching in −COOH) and at 1531 cm^{-1} (ionized carboxylate COO$^-$ asymmetric stretching). The PAH asymmetric NH$_3^+$ stretching band was also present at 1620 cm^{-1}. Bands attributed to covalent amide cross-linking were not observed (1540 and 1670 cm^{-1} carbonyl stretching in CONH amide bending).[38] These results confirm that PAH and PAA are both present in the sample, that they have some degree of ionization, and that they are not covalently cross-linked.

The degree of ionization (α) of PAA within PAH−PAA complexes was quantified using FTIR spectroscopy.[35,39] The degree of ionization and pK$_a$ of a weak polyelectrolyte can change strikingly from its pure solution state when assembled into multilayers or complexes.[15,39] The extinction coefficients of the ionized and not ionized forms of carboxylic acid were considered to be equal.[40,41] The absorbance (Abs) of −COOH

and COO$^-$ bands are related to α by the following expression:[39]

$$\alpha = \frac{Abs(COO^-)}{Abs(COO^-) + Abs(COOH)} \times 100\% \tag{1}$$

From this equation, the degree of ionization of PAA within PECs of pH 3.5, 5.5, 7, and 9 were 74%, 92%, 93%, and 95%, respectively (Figure 1b). As the complexation pH increases, α increases.

^{1}H NMR spectra of PAA, PAH, and complexes (Figure S2) were used to calculate the composition of the complexes. The PAA mol % (by repeat unit) was 62%, 56%, 53%, and 50% for complexes prepared from pH 3.5, 5.5, 7, and 9 solutions, respectively. As the pH of complexation increases, the amount of PAA in the complex decreases.

To establish the general behavior of *dried* PAH−PAA PECs, conventional DSC was performed on (PAH−PAA)$_{3.5}$ complexes (Figure 2a and Figure S3a). In the first heating cycle, two
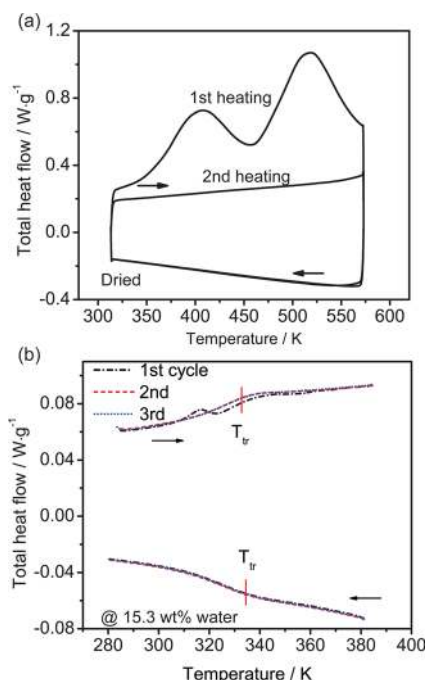

Figure 2. (a) Conventional DSC of dried (PAH−PAA)$_{3.5}$ complex at a scan rate of 10 K min^{-1} and (b) MDSC total heat flow of hydrated (PAH−PAA)$_{3.5}$ complex (15.3 wt % water) at a scan rate of 2 K min^{-1} with an amplitude of 1.272 K and a period of 60 s. All thermograms are shown in "exotherm down" format.

endothermic peaks at 406 and 516 K with a combined heat of 277 J g^{-1} were observed. These peaks did not appear in the second heating cycle, indicating that the observed endothermic processes were irreversible. This result is similar to the thermal behavior of dried PAH/PAA LbL films, in which the low-temperature peak was assigned to the loss of bound water and the high-temperature peak was assigned to amide cross-linking.[28] No glass transition-like behavior was observed in the dried complex.

The thermal behavior of *hydrated* PAH−PAA complexes was next investigated using MDSC. MDSC is different from traditional DSC because it applies superimposed sinusoidal (modulated) and linear heating rates. This separates the total heat flow into reversing and nonreversing heat flows depending

on the heat flow response. Heat capacity, melting, and glass transition events are observed in the "reversing heat flow" curve, and the "nonreversing heat flow" is associated with kinetic processes such as cross-linking and aging.[42] The "total heat flow" is the sum of the reversing and nonreversing heat flow, resembling the response of conventional DSC. MDSC was required here because the transitions observed were generally weak.

The total heat flow from MDSC of hydrated (PAH–PAA)$_{3.5}$ complex (15.3 wt % water) is shown in Figure 2b. A sigmoidal transition appears in all successive scans, for which the inflection point is assigned as the thermal transition temperature T_{tr}. Both second and third scans overlap, indicating reversible behavior. Figure S3b shows the corresponding reversing and nonreversing heat flows for the second heating scan. The sigmoidal transition is captured in the reversing heat flow, accompanied by enthalpic relaxation in the nonreversing heat flow as described by a broad, weak peak. For comparison, the dried complex exhibited none of these features (Figure S3a). As controls, hydrated homopolymers PAA and PAH (15.3 wt % water) were also examined (Figure S4); neither exhibited remarkable thermal features, consistent with prior reports.[37] These results demonstrate that the thermal transition is only observable for hydrated PAH–PAA complexes.

The effects of varying complexation pH and water content on T_{tr} were further examined using MDSC. Figure 3a shows a collection of reversing heat flow curves taken from the second heating scan for (PAH–PAA)$_{3.5}$ complexes with various added water content, where the subscript denotes the complexation pH. As the added water content increased from 15.3 to 24.2 wt %, T_{tr} decreased from 334 to 296 K. Figure 3b shows similar curves for the case of varying complexation pH values and constant added water content (15.3 wt %). As the complexation pH increased from pH 3.5 to 9, T_{tr} increased from 334 to 363 K. Figure 3c summarizes the observed T_{tr} for a matrix of added water content and complexation pH. The general observation is that T_{tr} decreases with decreasing complexation pH and increasing hydration.

Besides, T_{tr}, the enthalpic relaxation (ΔH, taken as the integrated area under the peak in the nonreversing heat flow), was examined as a function of complexation pH and added water content (Table S1). The value of ΔH ranged from 0.52 to 3.81 J/g, which is considered very small as compared to enthalpies of melting (188 J/g for poly(ethylene oxide)[43] but similar to enthalpies associated with a lower critical solution temperature (LCST)-type phase transitions (0.21−0.46 J/g for a N-isopropylacrylamide polymer hydrogel).[44] In general, ΔH decreased with increasing hydration, whereas no trend in complexation pH was observed.

The trends in Figure 3c are curious in that each curve has the same general shape and appear to be shifted from one another to some extent. To explore the possibility of any unifying controlling parameters, we attempted to collapse the data in Figure 3c into a master curve by plotting T_{tr} against various permutations of PAA ionization, PAH–PAA composition, and water content. Only when T_{tr} was plotted against the number of water molecules divided by the number of intrinsic ion pairs did the data successfully collapse into a single master curve (Figure 4a). Three assumptions were made to calculate the number of intrinsic ion pairs: (1) PAH degree of ionization was 100% from pH 3.5 to pH 9,[39] and (2) every PAH unit participated in intrinsic ion pairing. The former assumption is reasonable given that the pK_a's of polyelectrolytes tend to shift by as much as 2−
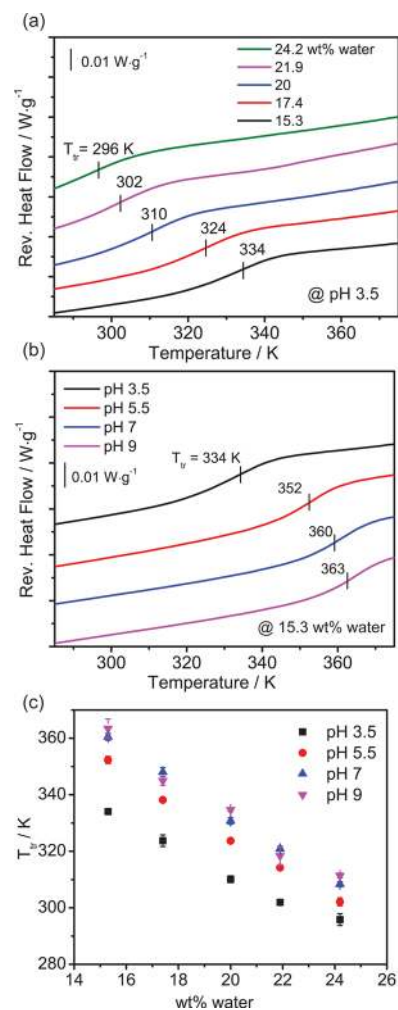

Figure 3. Reversing heat flows of (a) (PAH–PAA)$_{3.5}$ complexes of varying water content and of (b) varying complexation pH values and constant water content (15.3 wt % water). For (a) and (b), second heating scans are shown, and curves have been shifted along the y-axis for clarity. (c) T_{tr} for PAH–PAA complexes for varying complexation pH values and water content.

3 units upon complexation; PAH, normally having a pK_a of about 8.5, would thus shift to 10.5 or 11.5. This shift was clearly observed here for PAA using FTIR but due to overlapping peaks could not be clearly observed for PAH. (3) The number of water molecules was calculated as the total amount of water added to the PEC. A plot of ln(water/intrinsic ion pair) vs 1/T_{tr} yielded a straight line in the form of ln(water/intrinsic ion pair) = 1267.7(1/T_{tr}) − 3.18 (R^2 = 0.991) (Figure 4b). This presents an Arrhenius-type or Boltzmann energy distribution-type relationship, yielding an energy of −10.5 kJ/mol from the fitted slope. The meaning of this relationship is not yet perfectly clear and deserves more attention. The successful collapse of T_{tr} into a single master curve without any adjustable parameters is remarkable considering this has not been previously demonstrated and has strong implications on the role of water around intrinsic ion pairs for the thermal transition.

To further understand the role of water, we investigated PECs in the presence of water–solvent mixtures, specifically (PAH–PAA)$_{3.5}$ in the presence of 1-propanol and water. 1-Propanol has a boiling point close to that of water, and mixtures of 1-propanol and water lead to increased viscosity and
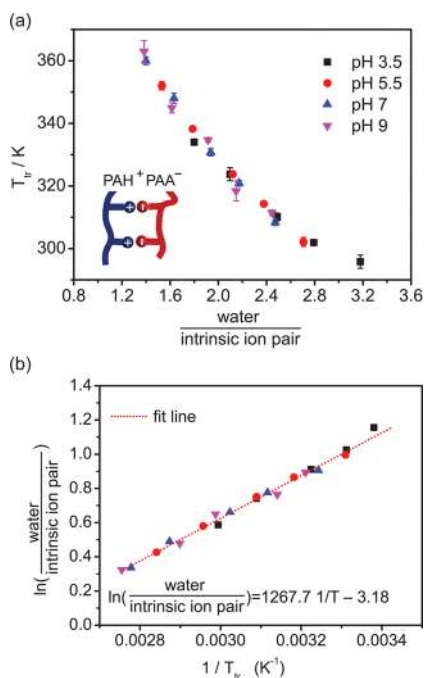
Figure 4. (a) T_{tr} vs number of water molecules per intrinsic ion pair in hydrated PAH−PAA PECs prepared at pH 3.5, 5.5, 7, and 9. The number of water molecules is taken as the total amount water added to the complex. The number of intrinsic ion pairs is calculated from the PEC mass and PAH−PAA composition, assuming that all PAH units are ionized and participate in intrinsic ion pairing. (b) Linear fitting of ln(water/intrinsic ion pair) vs $1/T_{tr}$. The legend in (a) also applies to (b).

decreased surface tension.[45] The T_g of water is 135 K,[46] and that of 1-propanol is 96.2 K.[47] The relative permittivity of water is 80.36 at 293 K,[48] and that of 1-propanol is 20.45 at 293 K.[49] Also, an individual water molecule can participate in hydrogen bonding at two sites, whereas 1-propanol can participate at one. Figure 5 shows T_{tr} for (PAH−PAA)$_{3.5}$ complexes in the presence of mixtures of varying water/1-propanol content and of varying added liquid content, where "liquid" stands for the
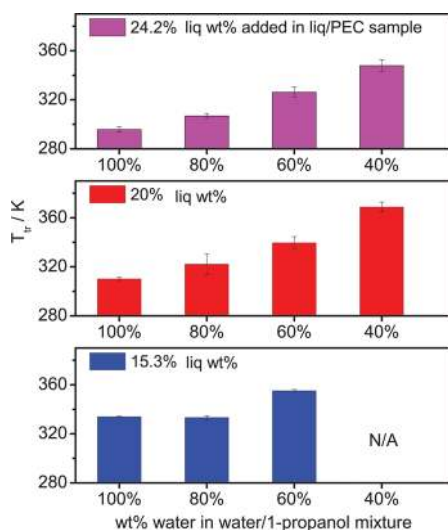

Figure 5. T_{tr} of (PAH−PAA)$_{3.5}$ complexes with varying water/1-propanol ratios and liquid to PEC ratio (where liquid denotes water and 1-propanol together).

combined water and 1-propanol mass. It is generally observed that T_{tr} increases with decreasing added liquid and with decreasing water content. For example, at a constant liquid content of 20 wt % (red bars, middle panel), T_{tr} increased from 310 to 369 K as the water content in the liquid decreased from 100 to 40 wt %. At high 1-propanol content, T_{tr} exceeded observable limits (labeled as N/A, bottom panel). This observation suggests that 1-propanol does not plasticize the complex.

To further investigate the role of hydrogen bonding in regard to the thermal transition, we measured T_{tr} in the presence of aqueous urea solution (Figure 6). Urea is known to compete
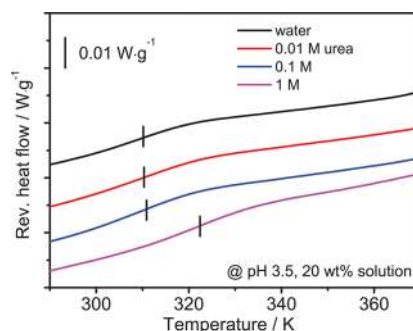

Figure 6. MDSC reversing heat flows of 20 wt % hydrated (PAH−PAA)$_{3.5}$ with water or with aqueous urea solution. Second heating scans are shown.

with hydrogen-bonding interactions and to slow water dynamics of water interacting with urea molecules.[50] The T_{tr} of (PAH−PAA)$_{3.5}$ at 20 wt % water was 310 K, whereas the T_{tr} for the PEC at equivalent aqueous urea solutions of 0.01, 0.1, and 1 M were 310, 311, and 322 K, respectively. As urea content increases, T_{tr} increases.

From the preceding, it is clear that increasing water content lowers T_{tr}. To further investigate the influence of water, we plot T_{tr} as a function of the water to PEC mass ratio in Figure 7
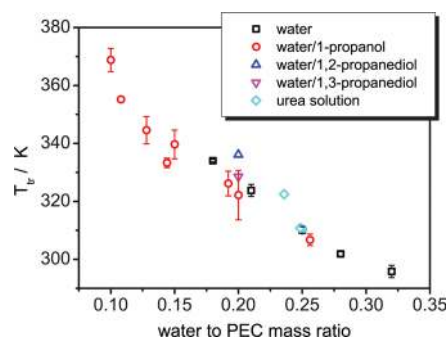
Figure 7. T_{tr} of (PAH−PAA)$_{3.5}$ complexes as a function of only water to PEC mass ratio for samples treated with water or other liquid mixtures.

where data are aggregated from (PAH−PAA)$_{3.5}$ complexes in the presence of pure water or other liquid mixtures. Because the preparation pH was kept constant at 3.5, the extent of intrinsic ion pairing is expected to remain constant. The water/PEC data are shown as black squares, water/1-propanol/PEC as red circles, and urea as cyan diamonds. We also investigated 1,2- and 1,3-propanediol (blue and purple triangles, respectively). Remarkably, the different sets of data overlap and follow a

general trend of T_{tr} decreasing with increasing water content. The fact that the data overlap regardless of whether 1-propanol or propanediol is present suggests that neither strongly affect T_{tr} and that the added solvents may not be interacting strongly with intrinsic ion pairs.

■ DISCUSSION

Complexes and LbL assemblies are often compared to one another because they are formed using the same interactions. In prior work,[37] we measured T_{tr} for PAH/PAA LbL assemblies as a function of assembly pH (and therefore composition). Table 1 compares these aspects for both LbL assemblies and

Table 1. Properties of Hydrated PAH/PAA LbL Films and Complexes (with 15.3 wt % Water)

pH	wt % PAA, LbL[a]	$T_{tr,LbL}$[a] (K)	wt % PAA, complexes	$T_{tr,complex}$ (K)
3.5	51 ± 3	335 ± 1	67 ± 1	334 ± 0.4
5.5	29 ± 2	324 ± 6	61 ± 1	352 ± 1
7.0	43 ± 1	N/A	58 ± 3	360 ± 1
9.0	15 ± 2	333 ± 10	55 ± 1	363 ± 3

[a]Data are taken from ref 37.

complexes. At a given pH, LbL assemblies and complexes have strikingly different compositions. This is most likely because the complexes were dialyzed for 4 days against a matching pH buffer solution, which may give longer time for equilibration.[16] In contrast, LbL assemblies are generally recognized as nonequilibrium structures.[51] Whereas complexes demonstrate a steady trend in T_{tr} with pH, LbL assemblies do not. Significantly, this comparison shows that T_{tr} depends on structure (composition) even if the assembly pH values are identical.

Also, these results show that complexation pH influences the degree of polyelectrolyte ionization in PAH−PAA complexes (Figure 1b). At pH 3.5, the degree of PAA ionization α in the complex was 74%, which is dramatically higher than that of spin-cast PAA (10%) and of PAA in an LbL assembly (45%) at equivalent conditions.[15,35] This suggests that PAA within the PAH−PAA complex has a very low pK_a (well below that of 3.5), which is lower than that of homopolymer PAA (pK_a = 5.5−6.5) and perhaps nearer to that of the LbL assembly (pK_a = 2.5−2.75).[15,52] This is because complexation lowers the ionization barrier for PAA.[15]

Complexation pH also influences the composition of the PAH−PAA complex. Although these are formed from stoichiometric (by repeat unit) mixtures, the resulting dialyzed complexes have compositions ranging from 62 to 50 mol % PAA as complexation pH increases from 3.5 to 9. This is because of mismatched degrees of ionization between PAA and PAH. At pH 3.5, PAA is partially ionized and PAH is fully ionized; therefore, more PAA must participate in complexation so as to fully neutralize PAH. Not until pH 7−9 does a stoichiometric mixture approach the composition of a stoichiometric complex. Similar behavior could be expected for LbL films, but the data of Table 1 show that the film composition does not comply with a systematic trend. As already noted, this is very likely due to LbL films being out-of-equilibrium.

The results show that water strongly affects the transition and appears to have a plasticizing effect by which T_{tr} decreases with increasing water content. Dried PAH−PAA complexes do

not exhibit any evidence of a T_g or T_{tr} because extensive intrinsic ion pairing lowers the mobility of polymer chain segments and raises T_{tr} outside of reasonable observation. As water is added to the PAH−PAA complex, we first observe the appearance of a T_{tr} at 15.3 wt % water. As more water is added, T_{tr} decreases further until it lies below our observation range (Figure 3a). Notably, homopolymer control samples hydrated with 15.3 wt % water yielded no thermal features (Figure S4). These results show that water is essential for the transition.

Water may exist in several forms within the PEC: as bulk water, water bound at extrinsic ion pairs (polyelectrolytes compensated by small counterions), and water bound at intrinsic ion pairs. Given the fairly low hydration levels we explored, we expect the latter two to be of more significance. The collapse of all T_{tr} into a single master curve when plotted against the ratio of added water to intrinsic ion pairs suggests that water at this site is very important to the transition. To test the validity of the water/intrinsic ion pair ratio, we also plot T_{tr} for PAA, PAH, water/extrinsic PAA sites, and water/neutral PAA sites in Figure S5. PAA units will exist in three distinct states: (1) ionized and intrinsically compensated, (2) ionized and extrinsically compensated, and (3) neutral. PAH is expected to exist as fully ionized and intrinsically compensated over the range of pH values studies. Only in the case of PAH is a master curve reproduced, consistent with our assumptions. Plotted another way, we show T_{tr} vs composition and vs PAA ionization at a constant hydration in Figure S6. T_{tr} generally increases with decreasing PAA composition and with increasing PAA ionization. In light of our findings, we attribute this trend to the general increase in the number of PAH$^+$−PAA$^-$ intrinsic ion pairs within the complex and the corresponding decrease in the number of water molecules per intrinsic ion pair. Ion pairs act as noncovalent cross-links and reduce chain mobility, thus increasing T_{tr}. As the composition approaches stoichiometric values (toward pH 9), the number of intrinsic ion pairs should increase, consistent with an increase in T_{tr} (Figure 3b,c).

In light of prior simulations[34] and the results presented here, water may play multiple roles in the thermal transition. Prior simulations of PDAC−PSS complexes indicate that the thermal transition is accompanied by a decrease in the number of water molecules surrounding the extrinsic PSS site and a change in the hydrogen-bonding water−polyelectrolyte network. On the other hand, the work presented here points to the role of water at the intrinsic (PAH$^+$−PAA$^-$) ion pair. It is possible that adding water to the PEC weakens this ion pair, meaning that the electrostatic interactions between PAH and PAA may be reduced. Consequently, the volume for chain relaxation increases with increasing hydration and water acts as a plasticizer, assisting with chain motion. Our past and current findings lead us to propose a two-step mechanism to describe the thermal transition observed in hydrated PECs: (1) water−polymer hydrogen bonding weakens first as temperature increases, and (2) this is followed by polymer chain relaxation facilitated by water at intrinsic ion pair sites.

This proposed mechanism is further supported by the results for water/solvent mixtures shown in Figure 7. The fact that these all water/solvent mixtures overlap for a graph of T_{tr} vs water/PEC mass indicates the transition is controlled by water and that the solvent is acting as a spectator. Possible reasons are that alcohol does not hydrate the polymer matrix and that less polyelectrolyte−water hydrogen bonds are formed as compared with pure water. The latter is supported by the fact that neither 1,2- nor 1,3-propanediol caused significant deviations from the

curve in Figure 7. With regard to urea, it was observed that increasing urea content increased T_{tr}. It may be interpreted as the ability of urea to disrupt hydrogen bonds,[50,53] thus reducing the "apparent" water content. However, no remarkable departure from the curve in Figure 7 was observed, so the results with urea may be interpreted similar to that of 1-propanol and the propanediols. Changes in the dielectric constant may also be considered, where the dielectric constant of 1-propanol is lower than that of water (20.45 vs 80.36 at 293 K), such that the Debye screening length is reduced in 1-propanol. As a consequence, water hydrating intrinsic ion pairs can be expected to weaken the Coulombic interaction between the ion pairs significantly in comparison to propanol as the solvent. Complementary results regarding water content have been observed for organic solvent and osmotic agents for PECs and with LbL assemblies, where deswelling and stiffening occur.[32,33,54,55]

CONCLUSION

The glass-transition-like thermal transition in polyelectrolyte complexes containing weak polyelectrolytes PAH and PAA was probed experimentally as a function of water content and complexation pH. Dried PAH−PAA PECs did not bear an observable T_{tr} in contrast to hydrated PECs. As the hydration content increased over a narrow range, T_{tr} decreased by tens of degrees. PECs prepared at lower pH values (pH 3.5) had a lower T_{tr} because of mismatching charge density, less ion pairs per unit volume, and higher PAA content. For PECs of (PAH−PAA)$_7$ and (PAH−PAA)$_9$, their composition and ionization were similar, which led to similar T_{tr} values. It was demonstrated that T_{tr} collapsed onto a single master curve when plotted against the ratio of water molecules to intrinsic ion pairs for all pH values investigated. The master curve demonstrated linearity when plotting ln(water/intrinsic ion pair) vs $(1/T_{tr})$. These results lead us to propose that the glass-transition-like thermal transition follows a two-step relaxation mechanism initiated with the weakening water−polymer interactions, followed by the relaxation of the polymer chains facilitated by water surrounding intrinsic ion pairs. Our future work will encompass molecular simulations to examine this proposed mechanism as well as further experimental investigation. In total, the implications of this study extend beyond dried PECs and are important to a range of areas related to water dynamics and influence on the polyelectrolyte systems including complexes and multilayers.

ASSOCIATED CONTENT

Ⓢ Supporting Information

The Supporting Information is available free of charge on the ACS Publications website at DOI: 10.1021/acs.macromol.6b00742.

> Digital images of PAH−PAA complexes; ^{1}H NMR spectra for pure PAA, PAH, and PAH−PAA complexes; MDSC thermograms of dried and hydrated (PAH−PAA)$_{3.5}$; MDSC thermograms of hydrated PAH, PAA, and water; relaxation energy of PAH−PAA complexes; T_{tr} with number of water molecules per PAA, PAH, extrinsic PAA, and neutral PAA repeat unit; T_{tr} as a function of PAA composition and PAA ionization (PDF)

AUTHOR INFORMATION

Corresponding Author

*E-mail: jodie.lutkenhaus@tamu.edu (J.L.L.).

Notes

The authors declare no competing financial interest.

ACKNOWLEDGMENTS

REFERENCES

(1) Michaels, A. S.; Miekka, R. G. Polycation-polyanion complexes: Preparation and properties of poly-(vinylbenzyltrimethylammonium) poly-(styrenesulfonate). *J. Phys. Chem.* **1961**, 65 (10), 1765−1773.

(2) Dautzenberg, H.; Schuldt, U. T. E.; Grasnick, G.; Karle, P.; MÜLler, P.; LÖHr, M.; Pelegrin, M.; Piechaczyk, M.; Rombs, K. V.; GÜNzburg, W. H.; Salmons, B.; Saller, R. M. Development of Cellulose Sulfate-based Polyelectrolyte Complex Microcapsules for Medical Applications. *Ann. N. Y. Acad. Sci.* **1999**, 875 (1), 46−63.

(3) Zhang, Y.; Yildirim, E.; Antila, H. S.; Valenzuela, L. D.; Sammalkorpi, M.; Lutkenhaus, J. L. The influence of ionic strength and mixing ratio on the colloidal stability of PDAC/PSS polyelectrolyte complexes. *Soft Matter* **2015**, 11 (37), 7392−7401.

(4) Perry, S. L.; Leon, L.; Hoffmann, K. Q.; Kade, M. J.; Priftis, D.; Black, K. A.; Wong, D.; Klein, R. A.; Pierce, C. F.; Margossian, K. O.; Whitmer, J. K.; Qin, J.; de Pablo, J. J.; Tirrell, M. Chirality-selected phase behaviour in ionic polypeptide complexes. *Nat. Commun.* **2015**, 6, 6052.

(5) Chollakup, R.; Smitthipong, W.; Eisenbach, C. D.; Tirrell, M. Phase Behavior and Coacervation of Aqueous Poly(acrylic acid)−Poly(allylamine) Solutions. *Macromolecules* **2010**, 43 (5), 2518−2528.

(6) Priftis, D.; Xia, X.; Margossian, K. O.; Perry, S. L.; Leon, L.; Qin, J.; de Pablo, J. J.; Tirrell, M. Ternary, tunable polyelectrolyte complex fluids driven by complex coacervation. *Macromolecules* **2014**, 47 (9), 3076−3085.

(7) van der Gucht, J.; Spruijt, E.; Lemmers, M.; Cohen Stuart, M. A. Polyelectrolyte complexes: Bulk phases and colloidal systems. *J. Colloid Interface Sci.* **2011**, 361 (2), 407−422.

(8) Nam, S. Y.; Lee, Y. M. Pervaporation and properties of chitosan-poly(acrylic acid) complex membranes. *J. Membr. Sci.* **1997**, 135 (2), 161−171.

(9) Kelly, K. D.; Schlenoff, J. B. Spin-Coated Polyelectrolyte Coacervate Films. *ACS Appl. Mater. Interfaces* **2015**, 7 (25), 13980−13986.

(10) Shamoun, R. F.; Hariri, H. H.; Ghostine, R. A.; Schlenoff, J. B. Thermal transformations in extruded saloplastic polyelectrolyte complexes. *Macromolecules* **2012**, 45 (24), 9759−9767.

(11) Shamoun, R. F.; Reisch, A.; Schlenoff, J. B. Extruded Saloplastic Polyelectrolyte Complexes. *Adv. Funct. Mater.* **2012**, 22 (9), 1923−1931.

(12) Chollakup, R.; Beck, J. B.; Dirnberger, K.; Tirrell, M.; Eisenbach, C. D. Polyelectrolyte Molecular Weight and Salt Effects on the Phase Behavior and Coacervation of Aqueous Solutions of Poly(acrylic acid) Sodium Salt and Poly(allylamine) Hydrochloride. *Macromolecules* **2013**, 46 (6), 2376−2390.

(13) Buchhammer, H.-M.; Mende, M.; Oelmann, M. Formation of mono-sized polyelectrolyte complex dispersions: effects of polymer structure, concentration and mixing conditions. *Colloids Surf., A* **2003**, 218 (1), 151−159.

(14) Dautzenberg, H.; Karibyants, N. Polyelectrolyte complex formation in highly aggregating systems. Effect of salt: response to subsequent addition of NaCl. *Macromol. Chem. Phys.* **1999**, 200 (1), 118−125.

(15) Boas, M.; Gradys, A.; Vasilyev, G.; Burman, M.; Zussman, E. Electrospinning polyelectrolyte complexes: pH-responsive fibers. *Soft Matter* **2015**, *11* (9), 1739−1747.

(16) Michaels, A. S. Polyelectrolyte complexes. *Ind. Eng. Chem.* **1965**, *57* (10), 32−40.

(17) Köhler, K.; Shchukin, D. G.; Möhwald, H.; Sukhorukov, G. B. Thermal Behavior of Polyelectrolyte Multilayer Microcapsules. 1. The Effect of Odd and Even Layer Number. *J. Phys. Chem. B* **2005**, *109* (39), 18250−18259.

(18) Köhler, K.; Möhwald, H.; Sukhorukov, G. B. Thermal Behavior of Polyelectrolyte Multilayer Microcapsules: 2. Insight into Molecular Mechanisms for the PDADMAC/PSS System. *J. Phys. Chem. B* **2006**, *110* (47), 24002−24010.

(19) Fortier-McGill, B.; Reven, L. 2H NMR Studies of Polymer Multilayer Capsules, Films, and Complexes. *Macromolecules* **2009**, *42* (1), 247−254.

(20) Zhou, J.; Pishko, M. V.; Lutkenhaus, J. L. Thermoresponsive layer-by-layer assemblies for nanoparticle-based drug delivery. *Langmuir* **2014**, *30* (20), 5903−5910.

(21) Sung, C.; Vidyasagar, A.; Hearn, K.; Lutkenhaus, J. L. Temperature-triggered shape-transformations in layer-by-layer microtubes. *J. Mater. Chem. B* **2014**, *2* (15), 2088−2092.

(22) Ibarz, G.; Dähne, L.; Donath, E.; Möhwald, H. Controlled Permeability of Polyelectrolyte Capsules via Defined Annealing. *Chem. Mater.* **2002**, *14* (10), 4059−4062.

(23) Köhler, K.; Shchukin, D. G.; Sukhorukov, G. B.; Möhwald, H. Drastic Morphological Modification of Polyelectrolyte Microcapsules Induced by High Temperature. *Macromolecules* **2004**, *37* (25), 9546−9550.

(24) Chen, D.; Chen, J.-T.; Glogowski, E.; Emrick, T.; Russell, T. P. Thin Film Instabilities in Blends under Cylindrical Confinement. *Macromol. Rapid Commun.* **2009**, *30* (4−5), 377−383.

(25) Mueller, R.; Köhler, K.; Weinkamer, R.; Sukhorukov, G.; Fery, A. Melting of PDADMAC/PSS Capsules Investigated with AFM Force Spectroscopy. *Macromolecules* **2005**, *38* (23), 9766−9771.

(26) Mueller, R.; Daehne, L.; Fery, A. Hollow Polyelectrolyte Multilayer Tubes: Mechanical Properties and Shape Changes. *J. Phys. Chem. B* **2007**, *111* (29), 8547−8553.

(27) Huglin, M. B.; Webster, L.; Robb, I. D. Complex formation between poly(4-vinylpyridinium chloride) and poly[sodium(2-acrylamido-2-methyl propane sulfonate)] in dilute aqueous solution. *Polymer* **1996**, *37* (7), 1211−1215.

(28) Shao, L.; Lutkenhaus, J. L. Thermochemical properties of free-standing electrostatic layer-by-layer assemblies containing poly (allylamine hydrochloride) and poly (acrylic acid). *Soft Matter* **2010**, *6* (14), 3363−3369.

(29) Jang, W.-S.; Jensen, A. T.; Lutkenhaus, J. L. Confinement Effects on Cross-Linking within Electrostatic Layer-by-Layer Assemblies Containing Poly(allylamine hydrochloride) and Poly(acrylic acid). *Macromolecules* **2010**, *43* (22), 9473−9479.

(30) Vidyasagar, A.; Sung, C.; Gamble, R.; Lutkenhaus, J. L. Thermal Transitions in Dry and Hydrated Layer-by-Layer Assemblies Exhibiting Linear and Exponential Growth. *ACS Nano* **2012**, *6* (7), 6174−6184.

(31) Sung, C.; Hearn, K.; Lutkenhaus, J. Thermal transitions in hydrated layer-by-layer assemblies observed using electrochemical impedance spectroscopy. *Soft Matter* **2014**, *10* (34), 6467−6476.

(32) Hariri, H. H.; Lehaf, A. M.; Schlenoff, J. B. Mechanical properties of osmotically stressed polyelectrolyte complexes and multilayers: Water as a plasticizer. *Macromolecules* **2012**, *45* (23), 9364−9372.

(33) Schlenoff, J. B.; Rmaile, A. H.; Bucur, C. B. Hydration contributions to association in polyelectrolyte multilayers and complexes: visualizing hydrophobicity. *J. Am. Chem. Soc.* **2008**, *130* (41), 13589−13597.

(34) Yildirim, E.; Zhang, Y.; Lutkenhaus, J. L.; Sammalkorpi, M. Thermal Transitions in Polyelectrolyte Assemblies Occur via a Dehydration Mechanism. *ACS Macro Lett.* **2015**, *4*, 1017−1021.

(35) Bieker, P.; Schönhoff, M. Linear and exponential growth regimes of multilayers of weak polyelectrolytes in dependence on pH. *Macromolecules* **2010**, *43* (11), 5052−5059.

(36) Shiratori, S. S.; Rubner, M. F. pH-Dependent Thickness Behavior of Sequentially Adsorbed Layers of Weak Polyelectrolytes. *Macromolecules* **2000**, *33* (11), 4213−4219.

(37) Vidyasagar, A.; Sung, C.; Losensky, K.; Lutkenhaus, J. L. pH-Dependent Thermal Transitions in Hydrated Layer-by-Layer Assemblies Containing Weak Polyelectrolytes. *Macromolecules* **2012**, *45* (22), 9169−9176.

(38) Harris, J. J.; DeRose, P. M.; Bruening, M. L. Synthesis of passivating, nylon-like coatings through cross-linking of ultrathin polyelectrolyte films. *J. Am. Chem. Soc.* **1999**, *121* (9), 1978−1979.

(39) Choi, J.; Rubner, M. F. Influence of the degree of ionization on weak polyelectrolyte multilayer assembly. *Macromolecules* **2005**, *38* (1), 116−124.

(40) Xie, A. F.; Granick, S. Local Electrostatics within a Polyelectrolyte Multilayer with Embedded Weak Polyelectrolyte. *Macromolecules* **2002**, *35* (5), 1805−1813.

(41) Sukhishvili, S. A.; Granick, S. Layered, Erasable Polymer Multilayers Formed by Hydrogen-Bonded Sequential Self-Assembly. *Macromolecules* **2002**, *35* (1), 301−310.

(42) Thomas, L. C. Modulated DSC Technology (MSDC-2006). TA Instruments, Inc. (www.tainstruments.com), New Castle, DE, 2006.

(43) Sung, C.; Vidyasagar, A.; Hearn, K.; Lutkenhaus, J. L. Effect of thickness on the thermal properties of hydrogen-bonded LbL assemblies. *Langmuir* **2012**, *28* (21), 8100−8109.

(44) Hu, C.-H.; Zhang, X.-Z.; Zhang, L.; Xu, X.-D.; Zhuo, R.-X. Temperature- and pH-sensitive hydrogels to immobilize heparin-modified PEI/DNA complexes for sustained gene delivery. *J. Mater. Chem.* **2009**, *19* (47), 8982−8989.

(45) Wang, Q.; Schlenoff, J. B. Single-and Multicompartment Hollow Polyelectrolyte Complex Microcapsules by One-Step Spraying. *Adv. Mater.* **2015**, *27* (12), 2077−2082.

(46) Hancock, B. C.; Zografi, G. The Relationship Between the Glass Transition Temperature and the Water Content of Amorphous Pharmaceutical Solids. *Pharm. Res.* **1994**, *11* (4), 471−477.

(47) Takahara, S.; Yamamuro, O.; Suga, H. Heat capacities and glass transitions of 1-propanol and 3-methylpentane under pressure. New evidence for the entropy theory. *J. Non-Cryst. Solids* **1994**, *171* (3), 259−270.

(48) Collie, C. H.; Hasted, J. B.; Ritson, D. M. The Dielectric Properties of Water and Heavy Water. *Proceedings of the Physical Society* **1948**, *60* (2), 145.

(49) Rana, V. A.; Vyas, A. D.; Mehrotra, S. C. Dielectric relaxation study of mixtures of 1-propanol with aniline, 2-chloroaniline and 3-chloroaniline at different temperatures using time domain reflectometry. *J. Mol. Liq.* **2003**, *102* (1−3), 379−391.

(50) Ilmain, F.; Tanaka, T.; Kokufuta, E. Volume transition in a gel driven by hydrogen bonding. *Nature* **1991**, *349* (6308), 400−401.

(51) Kim, B.-S.; Lebedeva, O. V.; Koynov, K.; Gong, H.; Glasser, G.; Lieberwith, I.; Vinogradova, O. I. Effect of organic solvent on the permeability and stiffness of polyelectrolyte multilayer microcapsules. *Macromolecules* **2005**, *38* (12), 5214−5222.

(52) Zacharia, N. S.; DeLongchamp, D. M.; Modestino, M.; Hammond, P. T. Controlling Diffusion and Exchange in Layer-by-Layer Assemblies. *Macromolecules* **2007**, *40* (5), 1598−1603.

(53) Aoki, T.; Kawashima, M.; Katono, H.; Sanui, K.; Ogata, N.; Okano, T.; Sakurai, Y. Temperature-Responsive Interpenetrating Polymer Networks Constructed with Poly(acrylic acid) and Poly-(N,N-dimethylacrylamide). *Macromolecules* **1994**, *27* (4), 947−952.

(54) Gu, Y.; Zacharia, N. S. Self-Healing Actuating Adhesive Based on Polyelectrolyte Multilayers. *Adv. Funct. Mater.* **2015**, *25* (24), 3785−3792.

(55) Gu, Y.; Ma, Y.; Vogt, B. D.; Zacharia, N. S. Contraction of weak polyelectrolyte multilayers in response to organic solvents. *Soft Matter* **2016**, *12* (6), 1859−1867.